# A Search for Short-Wavelength Neutrino Oscillation From a Nuclear Reactor

---

A Dissertation
Submitted to
the Temple University Graduate Board

---

In Partial Fulfillment
of the Requirements for the Degree
DOCTOR OF PHILOSOPHY

---

by
Danielle Berish Landschoot
December 2019

Examining Committee Members:

Darth Vader, Department of Physics, Advisory Chair
Luke Skywalker, Department of Physics
Han Solo, Department of Physics
Chew Bacca, Department of Physics
Lando Calrissian, External Reader, College of Engineering

# ABSTRACT

The Precision Reactor Oscillation and SPECTrum Experiment (PROSPECT) is designed to probe short baseline oscillations of antineutrinos in search of eV-scale sterile neutrinos and precisely measure the $^{235}$U reactor antineutrino spectrum from the High Flux Isotope Reactor (HFIR) at Oak Ridge National Laboratory. The PROSPECT antineutrino detector (AD) provides excellent background rejection and position resolution due to its segmented design and use of $^{6}$Li-loaded liquid scintillator. Due to characteristics of its decay chain, $^{227}$Ac was added as a calibration source that was dissolved isotropically throughout the liquid scintillator. Using the correlated production of alphas from $^{219}\text{Rn} \rightarrow {}^{215}\text{Po} \rightarrow {}^{211}\text{Pb}$ in the $^{227}$Ac decay chain we can measure the rate of $^{227}$Ac in each segment of the detector. This allows us to precisely determine the relative segment to segment volume variation to 1%. These measurements can then be applied as corrections to measurements of neutrino oscillation through the PROSPECT AD.

# ACKNOWLEDGEMENTS

These are the acknowledgements, where you express your appreciation to those who were influential and important to your success.

# TABLE OF CONTENTS

# LIST OF FIGURES

# LIST OF TABLES

# CHAPTER 1

# INTRODUCTION

# CHAPTER 2

# NEUTRINOS

## 2.1 Discovery of the Neutrino

The study of radioactive decay in the early 20th century exposed discrepancies that would lead to the postulation and eventual discovery of the neutrino. An experiment performed by Lise Meitner and Otto Hahn in 1911 offered some of the first evidence that the energy spectrum of electrons emitted by beta decay is continuous [3]. This was in stark contrast to the expected discrete spectra that had been observed in gamma and alpha emission, and suggested that the laws of conservation were broken during beta decay. Their findings were later confirmed by experiments performed by Chadwick in 1914 [4] and Ellis and Wooster in 1927 [5].

At the time, beta decay was thought to be a two-particle decay, a process that yields a product nucleus and an electron. In 1930, Wolfgang Pauli postulated a particle he called the 'neutron', which would be ejected with the electron, thereby conserving energy and momentum. Describing his idea as a "desperate remedy", this new particle would have to be neutral and non-interacting, therefore making it almost impossible to detect. In 1934, Enrico Fermi further developed the theory of beta decay, including Pauli's particle but renaming it the neutrino, meaning "little neutral one" [6]. Due to the nature of the weakly interacting neutrino, experimental discovery would take another 20 years.

In 1956 Clyde Cowan and Fred Reines accomplished the amazing feat of discovering this elusive particle experimentally by taking advantage of the inverse beta decay (IBD) process [7]:

$$\bar{\nu} + p \rightarrow n + e^{+} \tag{2.1}$$

Their idea was to place a detector near a generated flux of neutrinos, fill it with an ample number of protons, and observe the resulting positrons. However, any source that generates a large enough flux of neutrinos will create large backgrounds for the experiment. As would become the challenge for every neutrino detector thereafter, Cowan and Reines had to devise a way to reduce the background such that they could obtain a measurable and believable number of neutrinos. Their original idea was to place a detector underground about 40 meters away from a fission bomb. This would create a neutrino flux large enough to provide a sufficient signal to background ratio.

After some thought, though, they realized that by detecting the neutron *and* the positron they could discriminate the IBD signal from the background with much higher success. This would allow the use of a nuclear reactor instead of a fission bomb as a neutrino source, giving them the opportunity to patiently watch for neutrinos rather than be restricted to one chance with a bomb. The final detector that would facilitate the discovery of the electron anti-neutrino, $\bar{\nu_e}$, contained 1400 liters of liquid scintillator viewed by 110 photomultiplier tubes and 200 liters of water with dissolved cadmium chloride, and was placed near the fission reactor at the Savannah River Plant in South Carolina.

The mechanisms behind the detector developed by Cowan and Reines worked as follows. Neutrinos from the reactor enter the detector and interact with protons in the water. The positron resulting from this reaction quickly collides with an electron, creating two gamma rays which Compton scatter and initiate a cascade of electrons that causes the liquid to scintillate. Simultaneously, the neutron from the initial reaction bounces around as it collides with protons until, eventually, it captures on a cadmium nucleus and releases about a 9 MeV gamma ray, also causing the liquid to scintillate. The time between the flash of light from the positron annihilation and that of the neutron capture is on the order of microseconds. It was by looking for this delayed-coincidence signature that Cowan and Reines were able to successfully detect the first neutrino, and thus pave the way for future neutrino experiments.

Only 6 years after the discovery by Cowan and Reines, Lederman, Schwartz, and Steinberger discovered the muon neutrino, $\nu_\mu$ [8], but the discovery of the tau neutrino, $\nu_\tau$, by the DONUT (Direct Observation of the Nu Tau) experiment would not occur until 44 years later [9, 10].

| | Fermions | | | | Bosons | |
|---|---|---|---|---|---|---|
| | spin = 1/2 | | | | spin = 1 | spin = 0 |
| Generation | I | II | III | | Gauge Bosons | Scalar Bosons |
| Quarks | u | c | t | | g | H |
| | d | s | b | | $\gamma$ | |
| Leptons | e | $\mu$ | $\tau$ | | Z | |
| | $\nu_e$ | $\nu_\mu$ | $\nu_\tau$ | | W | |

**Table 2.1:** The Standard Model of particle physics, composed of fermions and their corresponding antiparticles, the force carries (gauge bosons), and the Higgs boson.

## 2.2 Neutrinos in the Standard Model and Beyond

The Standard Model (SM) of particle physics is the result of several decades of work by many scientists. It is a field theory that describes three of the four fundamental forces (electromagnetic, strong and weak), and classifies all known elementary particles as outlined in Table 2.1.

Classified in three generations of leptons, neutrinos exist in corresponding flavors, electron neutrinos ($\nu_e$), muon neutrinos ($\nu_\mu$), and tau neutrinos ($\nu_\tau$), to the electron (e), muon ($\mu$), and tau ($\tau$) leptons, respectively. For each of these flavors a corresponding antiparticle also exists, $\bar{\nu_e}, \bar{\nu_\mu}, \bar{\nu_\tau}$.

If neutrinos have exactly zero mass and travel at the speed of light, then by definition their helicity, or handedness, is a permanent property. Since experiments only measured left-handed neutrinos [11], it was assumed that all neutrinos in the SM were massless. As will be discussed in greater depth in Section 2.3, it was later experimentally discovered that neutrinos oscillate, or change flavors, indicating that at least two of the three neutrinos must have mass.

Their ability to oscillate arises from the fact that neutrinos exist as flavor eigenstates, $\nu_\alpha$: $\alpha = e, \mu, \tau$, where each flavor is a superposition of mass eigenstates, $\nu_i$: $i = 1, 2, 3$:

$$|\nu_\alpha\rangle = \sum_i U_{\alpha i} |\nu_i\rangle \tag{2.2}$$

where $U_{\alpha i}$ is the unitary Pontecorvo-Maki-Nakagawa-Sakata (PMNS) mixing matrix. The PMNS matrix relates flavor to mass eigenstates and can be written in factorized form as:

$$U = \begin{pmatrix} 1 & & \\ & c_{23} & s_{23} \\ & -s_{23} & c_{23} \end{pmatrix} \begin{pmatrix} c_{13} & & s_{13}e^{-i\delta} \\ & 1 & \\ -s_{13}e^{i\delta} & & c_{13} \end{pmatrix} \begin{pmatrix} c_{12} & s_{12} & \\ -s_{12} & c_{12} & \\ & & 1 \end{pmatrix} \begin{pmatrix} 1 & & \\ & e^{i\alpha} & \\ & & e^{i\beta} \end{pmatrix} \quad (2.3)$$

where $s_{ij} = \sin\theta_{ij}$ and $c_{ij} = \cos\theta_{ij}$, $\theta_{ij} = [0, \pi/2]$, $\delta = [0, 2\pi]$ is the Dirac charge parity (CP) violation phase, and $\alpha$ and $\beta$ are two Majorana CP violation phases.

As a neutrino, $\nu_\alpha$, propagates in time the mass eigenstates evolve differently (assuming that $m_1 \neq m_2 \neq m_3$), resulting in a new flavor state, $\nu_\beta$. Massive neutrinos move through time and space as

$$|\nu_i(x,t)\rangle = e^{-\frac{i}{\hbar}(E_i t - \vec{p}_i \cdot \vec{x})} |\nu_i(0,0)\rangle = e^{-i\phi} |\nu_i(0,0)\rangle \quad (2.4)$$

The flavor state $\alpha$ at some point in time and space can then be defined as:

$$|\nu_\alpha(x,t)\rangle = \sum_i U_{\alpha i} |\nu_i(x,t)\rangle = \sum_i U_{\alpha i} e^{-i\phi_i} |\nu_i(0,0)\rangle \quad (2.5)$$

Therefore, the oscillation probability that a neutrino produced as flavor $\nu_\alpha$ will be detected as flavor $\nu_\beta$ after traveling for a period of time is given by

$$\begin{aligned} P(\nu_\alpha \to \nu_\beta) &= |\langle \nu_\alpha(0,0) | \nu_\beta(x,t) \rangle|^2 \\ &= \left| \sum_i U^*_{\alpha i} e^{-i\phi_i} U_{\beta i} \right|^2 \\ &= \sum_i \sum_k U^*_{\alpha i} U_{\beta i} U_{\alpha k} U^*_{\beta k} e^{-i(\phi_i - \phi_k)} \end{aligned} \quad (2.6)$$

This is true for any number of neutrino generations, but for the sake of simplicity, consider the case of two neutrino oscillation. In this scenario the mixing matrix can be written as

$$U = \begin{pmatrix} U_{\alpha 1} & U_{\alpha 2} \\ U_{\beta 1} & U_{\beta 2} \end{pmatrix} = \begin{pmatrix} \cos\theta_{12} & \sin\theta_{12} \\ -\sin\theta_{12} & \cos\theta_{12} \end{pmatrix} \quad (2.7)$$

Therefore, the probability of oscillation is given by

$$\begin{aligned} P^{2\nu}(\nu_\alpha \to \nu_\beta) &= |U_{\alpha 1}|^2 |U_{\beta 1}|^2 + |U_{\alpha 2}|^2 |U_{\beta 2}|^2 + U^*_{\alpha 1} U_{\beta 1} U_{\alpha 2} U^*_{\beta 2} (e^{i(\phi_2 - \phi_1)} + e^{-i(\phi_2 - \phi_1)}) \\ &= \sin^2 2\theta_{12} \sin^2 \left( \frac{\phi_2 - \phi_1}{2} \right) \end{aligned} \tag{2.8}$$

Now, recall that

$$\phi_i = \frac{1}{\hbar}(E_i t - \vec{p}_i \cdot \vec{x}) \tag{2.9}$$

The mass of the neutrino is very small compared to its energy ($m_\nu << E_\nu$) so the momentum can be approximated as

$$p_i = \frac{1}{c}\sqrt{E_i^2 - m_i^2 c^4} = \frac{1}{c}\left( E_i - \frac{m_i^2 c^4}{2E_i} \right) \tag{2.10}$$

If it is reasonably assumed that neutrinos move at the speed of light, $c$, then the phase difference, $\phi_2 - \phi_1$, can be approximated as

$$\begin{aligned} \phi_2 - \phi_1 &= \frac{1}{\hbar}\left( (E_2 - E_1)\frac{L}{c} - (p_2 - p_1)L \right) \\ &= \frac{1}{\hbar}\frac{L}{c}\left( \frac{m_2^2 c^4}{2E_2} - \frac{m_1^2 c^4}{2E_1} \right) \\ &= \frac{L}{\hbar c}\frac{\Delta m_{21}^2 c^4}{2E} \end{aligned} \tag{2.11}$$

where $t = \frac{L}{c}$, $\Delta m_{21}^2 = m_2^2 - m_1^2$ and $E_1 = E_2 = E$.

It can now be shown that the oscillation probability of a neutrino $\nu_\alpha$, being detected as flavor $\nu_\beta$ in the two neutrino mixing case is

$$P^{2\nu}(\nu_\alpha \to \nu_\beta) = \sin^2(2\theta_{12}) \sin^2 \left( \frac{c^4}{4\hbar c}\frac{\Delta m_{12}^2 L}{E} \right) \tag{2.12}$$

The corresponding survival probability, the chance that a neutrino $\nu_\alpha$ is detected as $\nu_\alpha$, can be described by $P^{2\nu}(\nu_\alpha \to \nu_\alpha) = 1 - P^{2\nu}(\nu_\alpha \to \nu_\beta)$.

There are several aspects of note about this probability. It can be seen that the amplitude of the oscillation probability, $\sin^2(2\theta_{12})$, depends on the mixing angle $\theta_{12}$,

while the mass splitting, $\Delta m^2_{12}$, the energy of the neutrino, $E$, and the distance traveled, $L$, determine the frequency of oscillation. The probability is non-zero only when $\Delta m^2_{12}$ is non-zero, indicating that if an experiment observes neutrino oscillation, then at least one of the neutrinos must have mass. Finally, the dependence of oscillation on the factor $\frac{L}{E}$ allows experiments to decide the placement of neutrino detectors based on what features of neutrinos they would like to study. Theoretical models alone do not prove neutrino oscillation, however. The first experimental evidence for oscillation and neutrino mass will be described in Section 2.3.

## 2.3 Discovery of Neutrino Oscillation

In the late 1960's, about a decade after Cowan and Reines discovered the first neutrino, astrophysicists Raymond Davis and John Bahcall designed an experiment to collect and count solar neutrinos, neutrinos emitted by nuclear fusion taking place in the Sun. Davis placed a 380 cubic meter tank filled with perchloroethylene (dry-cleaning fluid) 1,478 meters underground in the Homestake Gold Mine in South Dakota. Perchloroethylene was chosen because it is rich in chlorine and the tank was placed deep underground to shield the experiment from cosmic rays.

Davis was looking for the reaction

$$\nu_{\mathrm{e}} + {}^{37}\mathrm{Cl} \rightarrow {}^{37}\mathrm{Ar} + \mathrm{e}^- \tag{2.13}$$

in which a neutrino would enter the tank and transform chlorine into argon, which he would then extract and count. In the end, with the Homestake experiment Davis calculated a rate of solar neutrinos that was one third of the rate predicted by calculations made by Bahcall using the Standard Model [12]. This discrepancy became known as the solar neutrino problem, and in the following years Bruno Pontecorvo wrote several theoretical papers proposing neutrino oscillation as a solution [13, 14].

Several experiments designed to calculate the flux of solar neutrinos followed the Homestake Experiment including SAGE [15], GALLEX [16], and GNO [17, 18]. All three experiments built detectors based on the reaction ${}^{71}\mathrm{Ga}(\nu, \mathrm{e}^-){}^{71}\mathrm{Ge}$, and all three experiments showed a deficit in neutrino flux compared to Standard Model calculations.

Further experimental proof of neutrino oscillation came with results from the Super-Kamiokande Experiment. Unlike previous experiments that were only sensi-

| Parameter | Best-fit | $3\sigma$ |
|---|---|---|
| $\Delta m^2_{21}$ [$10^{-5}$ eV$^2$] | 7.37 | 6.93 - 7.96 |
| $\Delta m^2_{31(23)}$ [$10^{-3}$ eV$^2$] | 2.56 (2.54) | 2.45 - 2.69 (2.42 - 2.66) |
| $\sin^2\theta_{12}$ | 0.297 | 0.250 - 0.354 |
| $\sin^2\theta_{23}$ | 0.425 (0.589) | 0.381 - 0.615 (0.384 - 0.636) |
| $\sin^2\theta_{13}$ | 0.0215 (0.0216) | 0.0190 - 0.0240 (0.0190 - 0.0242) |
| $\delta/\pi$ | 1.38 (1.31) | $2\sigma$: 1.0 - 1.9 ($2\sigma$: 0.92 - 1.88) |

**Table 2.2:** The current best-fit values and $3\sigma$ allowed ranges of the 3-neutrino oscillation parameters as determined experimentally [22]. The values (values in brackets) correspond to $m_1 < m_2 < m_3$ ($m_3 < m_1 < m_2$).

tive to electron neutrinos, Super-K detected neutrinos through elastic scattering of electrons - a process sensitive to all neutrino flavors. With their large mass, good energy resolution, and ability to determine neutrino directionality, Super-K was able to confirm the solar neutrino problem effect with high statistics and place limits on the parameters of oscillation [19].

The first direct evidence for solar neutrino flavor change came from the Sudbury Neutrino Observatory (SNO) in 2001 [20, 21]. The SNO detector was an imaging Cherenkov detector using heavy water. They were able to observe neutrino flavor change through three different processes (elastic scattering of electrons, the $\nu_e - d$ charged current reaction, and the $\nu_x - d$ neutral current interaction) that, combined, were sensitive to all three neutrino flavors.

Nearly a century after the initial postulation of the neutrino the scientific community has in hand experimental evidence of three neutrino flavors, mathematical models that include these neutrinos in the Standard Model of Particle Physics, and theoretical and experimental proof that neutrinos oscillate and therefore have mass. These findings, along with developments in technology and techniques, set the stage for current, and future, neutrino experiments to transform their goals from observing anomalies to making precise measurements of the physics behind the anomalies. The current best-fit values of the 3-neutrino oscillation parameters as found experimentally are shown in Table 2.2.

# CHAPTER 3

# REACTOR NEUTRINOS

Nuclear reactors are a pure source of electron antineutrinos, $\bar{\nu}_e$, as a result of the fission of isotopes used in the reactor fuel. The first neutrino was discovered using the nuclear reactor at the Savannah River Plant, and reactor sites continue to be popular homes for neutrino detectors. In order to perform precision reactor neutrino studies it is important to understand the reactor neutrino flux and spectrum.

## 3.1 Production of Reactor Neutrinos

Nuclear reactors are powered by the fission of Uranium and Plutonium isotopes in their cores. Specifically, in a power reactor, 99.9% of the power comes from the fission of $^{235}$U, $^{239}$Pu, $^{241}$Pu, and $^{238}$U isotopes. The chain reaction begins with a neutron colliding with a nucleus of one of the isotopes. This causes the nucleus to split into two fragments, usually of unequal mass, creating an unstable system. In order to reach stability neutrons have to transform into protons, a process only accomplished through $\beta$ decay, see Figure 3.1. Each beta decay produces an electron and corresponding electron antineutrino. In general a nuclear reactor will produce $\sim 6 \times 10^{20} \bar{\nu}_e$ per GW of thermal energy power [2].

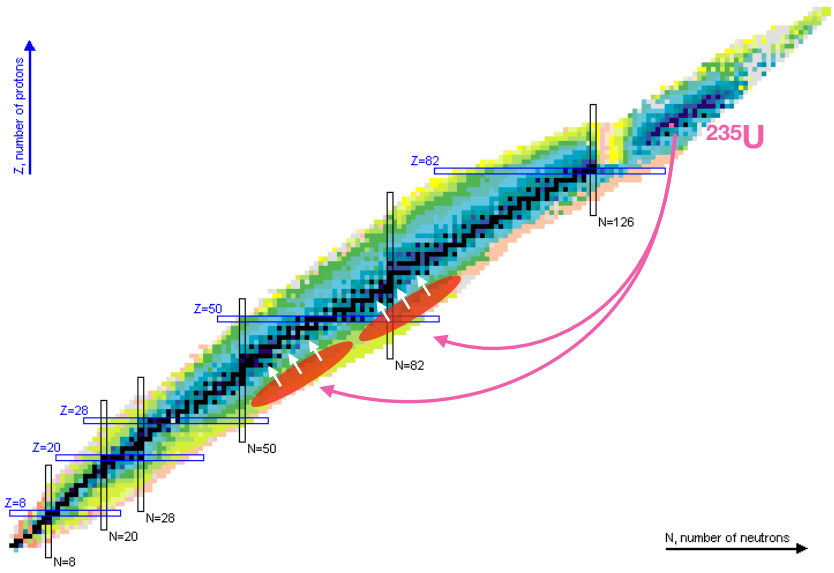


**Figure 3.1:** A schematic of the fission of $^{235}$U [1]. After collision with a neutron $^{235}$U will split into two unstable nuclei (pink arrows) which will then $\beta$ decay (white arrows) until stable.

## 3.2 Measuring the Reactor Antineutrino Flux and Spectrum

The total antineutrino spectrum produced by a nuclear reactor can be expressed as the sum over the spectra for the dominant fissioning isotopes,

$$S(E_\nu) = \frac{W_{th}}{\sum_i (f_i/F) e_i} \sum_i \frac{f_i}{F} \left( \frac{dN_i}{dE_\nu} \right), \tag{3.1}$$

where $f_i$ is the number of fissions from isotope $i$, $F$ is the total number of fissions, $W_{th}$ is the total reactor thermal energy, $e_i$ is the effective thermal energy per fission contributed by each isotope $i$, and $dN_i/dE_\nu$ is the cumulative $\bar{\nu}_e$ spectrum of $i$ normalized per fission.

There are two methods to determine the $\bar{\nu}_e$ spectrum, *ab initio* summation and electron spectrum conversion. In the *ab initio* approach the spectrum is determined by summing the contributions of all $\beta$-decay branches of all fission fragments,

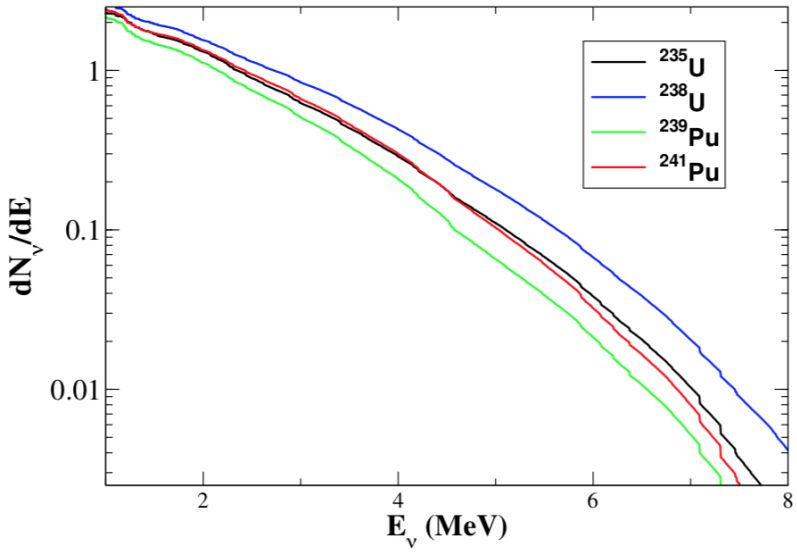


**Figure 3.2:** The $\bar{\nu}_e$ spectrum predicted by the summation method using the JEFF-3.1.1 database fission fragment yields and the ENDF/B-VII.1 decay library [2].

$$\frac{dN_i}{dE_{\bar{\nu}}} = \sum_n Y_n(Z, A, t) \sum_{n,i} b_{n,i}(E_0^i) P_{\bar{\nu}}(E_{\bar{\nu}}, E_0^i, Z), \tag{3.2}$$

where $Y_n(Z, A, t)$ is the number of $\beta$ decays of the fission fragment $Z, A$ at time $t$, $b_{n,i}(E_0^i)$ are the branching ratios with endpoint energies $E_0^i$, and $P_{\bar{\nu}}(E_{\bar{\nu}}, E_0^i, Z)$ is the normalized $\bar{\nu}_e$ spectrum for the branch $n, i$. The antineutrino spectrum for the four main reactor isotopes calculated using this method can be seen in Figure 3.2. Unfortunately, with this method comes several sources of uncertainty. The fission yields, $Y_n$ have been determined by a few different groups, but don't always agree and have large uncertainties and not all branching ratios are known. For this reason another method can be considered.

The electron spectrum conversion method involves converting a measured electron spectrum into an antineutrino spectrum. This involves fitting an experimentally defined total beta spectrum with individual beta spectrum according to their amplitudes, $a_i$,

$$\frac{dN_i}{dE_e} = \sum_i a_i P(E, E_0^i, Z) \tag{3.3}$$

The conversion to the antineutrino spectrum is then accomplished by replacing

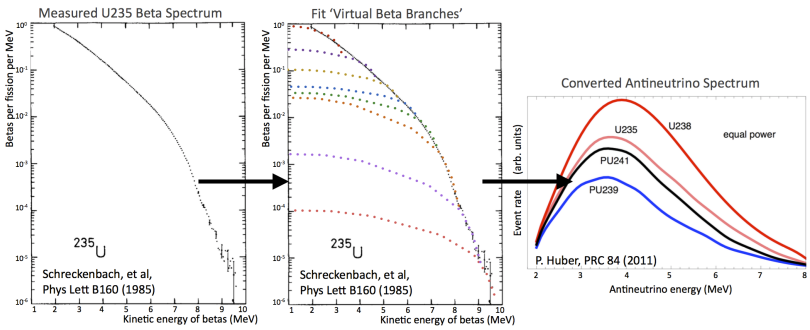


**Figure 3.3**

the energy $E_e$ in each branch by $E_0 - E_{\bar{\nu}}$, because the electron and the $\bar{\nu}_e$ share the total energy of each $\beta$-decay branch. The flux per fission is then given as the sum of $\bar{\nu}_e$ spectrum converted from each virtual $\beta$ branch,

$$\frac{dN_i}{dE_{\bar{\nu}}} = \sum_i a_i P(E_0^i - E, E_0^i) \tag{3.4}$$

[**New figure?**]

## 3.3 Detection of Reactor Neutrinos

Though there are several methods that can be used to detect reactor neutrinos, including charge-current ($\bar{\nu}_e + d \to n + n + e^+$), neutral-current ($\bar{\nu}_e + d \to n + p + \bar{\nu}_e$), and antineutrino-electron elastic scattering ($\bar{\nu}_e + e^- \to \bar{\nu}_e + e^-$), the one employed by most experiments is IBD ($\bar{\nu}_e + p \to e^+ + n$). The IBD reaction energy threshold is 1.8 MeV and the cross section is relatively high, $\sim 63 \times 10^{-44}\text{cm}^2$/fisson integrated over the entire reactor neutrino energy spectrum [23], and can be written as

$$\sigma^{(0)} \simeq 9.52 \times \left( \frac{E_e^{(0)} p_e^{(0)}}{\text{MeV}^2} \right) \times 10^{-44}\text{cm}^2 \tag{3.5}$$

where $E_e$ and $p_e$ are the energy and momentum of the final-state positron.

An IBD event is selected by a pair of coincident signals consisting of a positron ionization and annihilation as the prompt signal and a time delayed neutron capture on a proton or nucleus as the delay signal. The neutron energy can be backtracked

from the prompt signal as

$$E_{\bar{\nu}} = E_{prompt} + 0.78 \text{ MeV} + T_n \tag{3.6}$$

where $T_n$ is the kinetic energy of the recoil neutron which is much smaller than the energy of the neutrino and can therefore be ignored in most cases. The IBD cross-section increases with energy, whereas the $\bar{\nu}_e$ spectrum decreases with energy creating a detected energy spectrum that peaks around 3.8 MeV and dies off after ∼8 MeV, as seen in Figure 3.4.

In addition to great background rejection and good reconstruction of the neutrino energy, the IBD method of detecting neutrinos also allows the use of liquid scintillators and water as detection mediums.

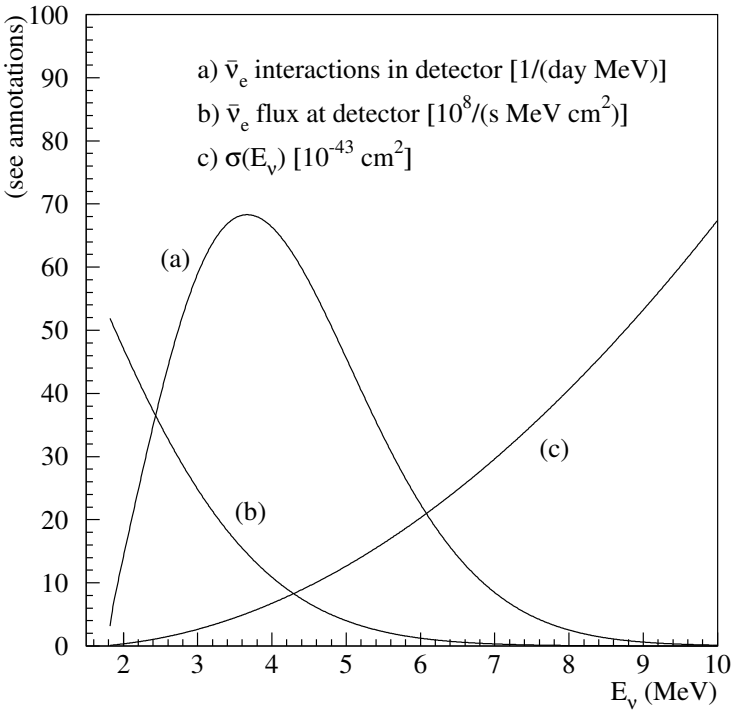


**Figure 3.4:** The IBD spectrum (curve (a)) measured by a 12-ton fiducial mass detector located 0.8 km from a 12-GW$_{th}$ power reactor along with the reactor flux (curve (b)) and IBD cross section (curve (c)) as a function of energy [22].

## 3.4 The Reactor Antineutrino Anomaly

# CHAPTER 4

# STERILE NEUTRINOS

## 4.1 Theory of Sterile Neutrinos

## 4.2 Experimental Searches for Sterile Neutrinos

# CHAPTER 5

# PROSPECT

## 5.1 Motivation

## 5.2 Experimental Site

## 5.3 Design

## 5.4 Detecting Inverse Beta Decays

## 5.5 From Signal to Result

# CHAPTER 6

# $^{227}$AC AS A CALIBRATION SOURCE

## 6.1 Motivation

## 6.2 Material Compatibility

## 6.3 Prototype Testing in P50X

## 6.4 Event Selection in the PROSPECT AD

## 6.5 Detector Stability Results

## 6.6 Volume Variation Results

# CHAPTER 7

# INVERSE BETA DECAY EVENT SELECTION

## 7.1 Selection Criteria and Efficiency

## 7.2 Properties of the Event Selection

# CHAPTER 8

# NEUTRINO OSCILLATION IN THE PROSPECT AD

## 8.1 Analysis Method

## 8.2 Result

# CHAPTER 9

# CONCLUSIONS

.

# BIBLIOGRAPHY


[1] NNDC. Chart of Nuclides.

[2] A. C. Hayes and Petr Vogel. Reactor Neutrino Spectra. *Ann. Rev. Nucl. Part. Sci.*, 66:219–244, 2016.

[3] L Meitner O von Baeyer, O Hahn. Uber die -Strahlen des aktiven Niederschlags des Thoriums. *Zeitschrift fur Physik*, 12:273–279, 1911.

[4] J. Chadwick. The intensity distribution in the magnetic spectrum of beta particles from radium (B + C). *Verh. Phys. Gesell.*, 16:383–391, 1914.

[5] C. D. Ellis and W. A. Wooster. The average energy of disintegration of radium E. *Proceedings of the Royal Society of London Series A*, 117:109–123, 1927.

[6] E. Fermi. An attempt of a theory of beta radiation. 1. *Z. Phys.*, 88:161–177, 1934.

[7] C. L. Cowan, F. Reines, F. B. Harrison, H. W. Kruse, and A. D. McGuire. Detection of the free neutrino: a confirmation. *Science*, 124(3212):103–104, 1956.

[8] G. Danby, J-M. Gaillard, K. Goulianos, L. M. Lederman, N. Mistry, M. Schwartz, and J. Steinberger. Observation of high-energy neutrino reactions and the existence of two kinds of neutrinos. *Phys. Rev. Lett.*, 9:36–44, Jul 1962.

[9] K. Kodama et al. Observation of tau neutrino interactions. *Phys. Lett.*, B504:218–224, 2001.

[10] K. Kodama et al. Final tau-neutrino results from the donut experiment. *Phys. Rev. D*, 78:052002, Sep 2008.

[11] M. Goldhaber, L. Grodzins, and A. W. Sunyar. Helicity of neutrinos. *Phys. Rev.*, 109:1015–1017, Feb 1958.

[12] Raymond Davis, Don S. Harmer, and Kenneth C. Hoffman. Search for neutrinos from the sun. *Phys. Rev. Lett.*, 20:1205–1209, May 1968.

[13] B. Pontecorvo. Neutrino Experiments and the Problem of Conservation of Leptonic Charge. *Sov. Phys. JETP*, 26:984–988, 1968. [Zh. Eksp. Teor. Fiz.53,1717(1967)].

[14] S M Bilen'ki and Bruno Pontecorvo. Lepton mixing and neutrino oscillations. *Soviet Physics Uspekhi*, 20(10):776, 1977.

[15] J. N. Abdurashitov et al. Results from SAGE. *Phys. Lett.*, B328:234–248, 1994.

[16] W. Hampel et al. GALLEX solar neutrino observations: Results for GALLEX IV. *Phys. Lett.*, B447:127–133, 1999.

[17] M. Altmann et al. GNO solar neutrino observations: Results for GNO I. *Phys. Lett.*, B490:16–26, 2000.

[18] E. Bellotti. First results from GNO. *Nucl. Phys. Proc. Suppl.*, 91:44–49, 2001. [,44(2001)].

[19] Y. Fukuda et al. Evidence for oscillation of atmospheric neutrinos. *Phys. Rev. Lett.*, 81:1562–1567, Aug 1998.

[20] Q. R. Ahmad et al. Measurement of the rate of $\nu_e + d \rightarrow p + p + e^-$ interactions produced by $^8b$ solar neutrinos at the sudbury neutrino observatory. *Phys. Rev. Lett.*, 87:071301, Jul 2001.

[21] Q. R. Ahmad et al. Direct evidence for neutrino flavor transformation from neutral-current interactions in the sudbury neutrino observatory. *Phys. Rev. Lett.*, 89:011301, Jun 2002.

[22] M. Tanabashi et al. Review of particle physics. *Phys. Rev. D*, 98:030001, Aug 2018.

[23] Xin Qian and Jen-Chieh Peng. Physics with Reactor Neutrinos. *Rept. Prog. Phys.*, 82(3):036201, 2019.

# APPENDIX A

# SOME ADDITIONAL STUFF

Appendices go at the end.

# APPENDIX B

# MORE ADDITIONAL STUFF

This is another appendix.